Supporting Information

Multi-Functional Applications of a Metal-Free Viologen Supramolecular Compound: UV Detection, Amine Sensing, and Ink-Free Printing

Li Li [a,*] Chun-Jie Liu[a], Hang-Hang Guo[a], Ning-Ning Zhang[b], Hong-Li Wang[a]

1. Contents

1. Experimental Procedures

1.1. Materials

1-((4′-carboxy-[1,1′-biphenyl]-4-yl)methyl)-[4,4′-bipyridin]-1-ium[(cbmby)Br] was synthesized according to the literature method.[1] H_4betc was purchased from commercial sources and used without further purification. Water was deionized before use.

1.2. General instruments

A CEL-HXF300-T3 xenon lamp (ca. 110 mW/cm^2) was used to prepare irradiated samples for powder X-ray diffraction (PXRD), UV-vis spectroscopy, electron paramagnetic resonance (EPR) and time-dependent steady-state emission spectra. PXRD patterns were collected on a Rigaku Corporation SmartLab 9 kW diffractometer using Mo K_α radiation (λ = 0.71073 Å). Simulated PXRD patterns were derived from the Mercury program freely downloaded from the Cambridge Crystallographic Data Centre (CCDC; https://ccdc.cam.ac.uk/support-and-resources/downloads/). FT-IR spectra were measured by a PerkinElmer STA8000 Frontier IR spectrometer. UV-vis spectra were measured at room temperature on a Shimadzu UV-2600i spectrophotometer with an integrating sphere attachment and $BaSO_4$ as a reference. EPR spectra were recorded on a CIQTEK EPR-200Plus electron paramagnetic resonance spectrometer with a 100 kHz magnetic field in the X band. The photoluminescence (PL) emission (Em) spectra and PL excitation (Ex) spectra, tests were carried out on an Edinburgh FLS1000 UV/Vis/NIR Fluorescence Spectrometer.

1.3. Syntheses

1.3.1 Synthesis of (cbmby)(H_3betc)·H_2O (1)

(cbmby)Br (0.1 mmol, 36.7 mg) and H_4betc (0.1 mmol, 25.4 mg) were added to a 50 mL beaker, followed by the addition of 4 mL of H_2O and 4 mL of CH_3CN with stirring. After stirring for 30 min, a colorless and clear solution was obtained. The solution was transferred to a high-pressure reaction vessel with

a polytetrafluoroethylene liner, heated at 100 °C for 48 h, and then cooled to room temperature at a rate of 5 °C/h. After the reaction was completed, the product was rinsed and filtered using a mixture of deionized water and acetonitrile, ultimately yielding colorless, transparent rod-shaped crystals.

1.4. X-ray crystallography

Single-crystal X-ray diffraction measurement of **1** was performed on a Bruker Apex CCD D8 VENTURE diffractometer, using graphite-monochromated Mo-*Kα* radiation (λ = 0.71073 Å) at 273 K. The crystal structure was solved by the direct method and refined through a full-matrix least-square technique on F^2 using the Olex2 package.[2] All hydrogen atoms were treated with a riding model. All non-hydrogen atoms were refined anisotropically.

1.5. Theoretical calculation

The density functional theory (DFT) calculations were carried out using the Materials Studio software. Geometry Optimization and Energy modules within the Dmol3 software package were employed to perform structural and energetic optimizations. The Perdew-Burke-Ernzerh of generalized gradient approximation (PBE-GGA) were applied to analog electrostatic surfaces potential (ESP) and orbitals of polymer fragments .[3, 4] Utilize a cutoff energy threshold of 1.0×10^{-6} Hartree, a cutoff stress criterion of 0.001 Hartree per angstrom, and a cutoff displacement limit of 0.005 angstroms. The energy convergence criterion should be set to 1.0×10^{-6} Hartree, with a maximum number of optimization cycles capped at 500. The HOMO and LUMO orbitals of a structural fragment, extracted from **1** crystal structure, were all calculated at the B3LYP/6-311G** level using the Gaussian 16 program,[5] and analyzed by Multiwfn.[6]

2. Additional Figures

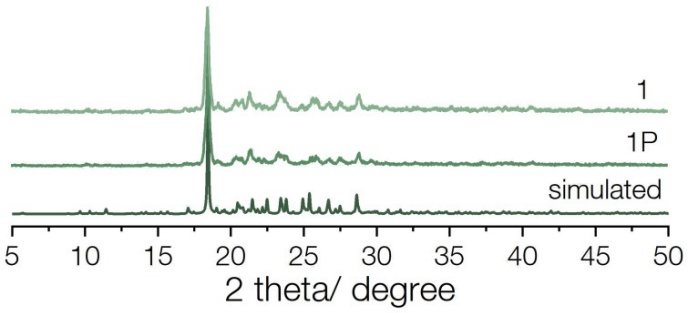

Fig. S1 Simulated and measured PXRD patterns for **1** and **1P**.

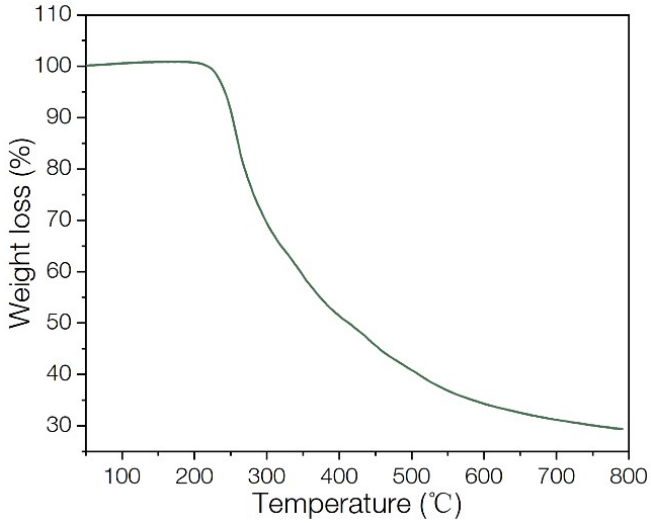

Fig. S2 The thermogravimetric curves of **1**.

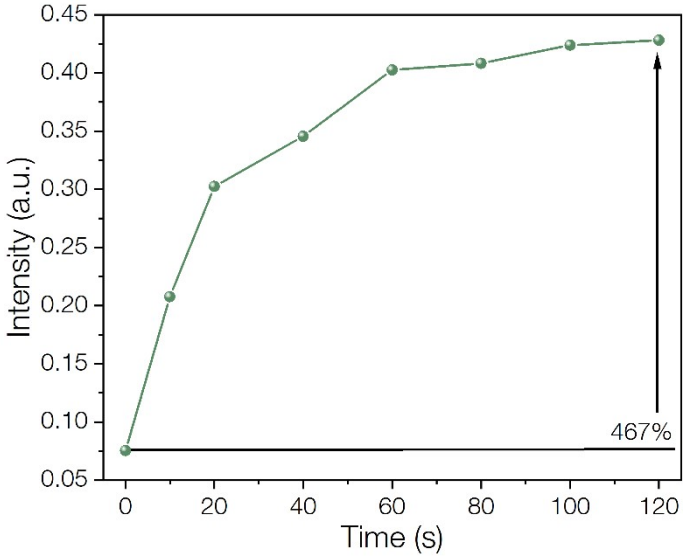

Fig. S3 The relative absorption change rate of **1** at 616 nm.

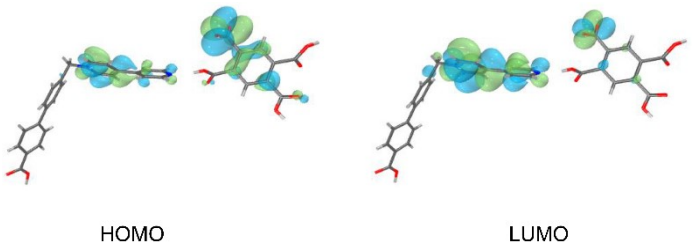

Fig. S4 Calculated molecular orbitals of **1**.

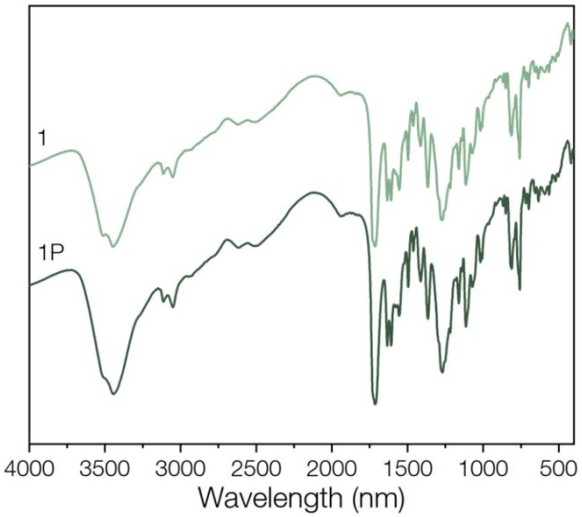

Fig. S5 IR spectra of **1** before and after irradiation.

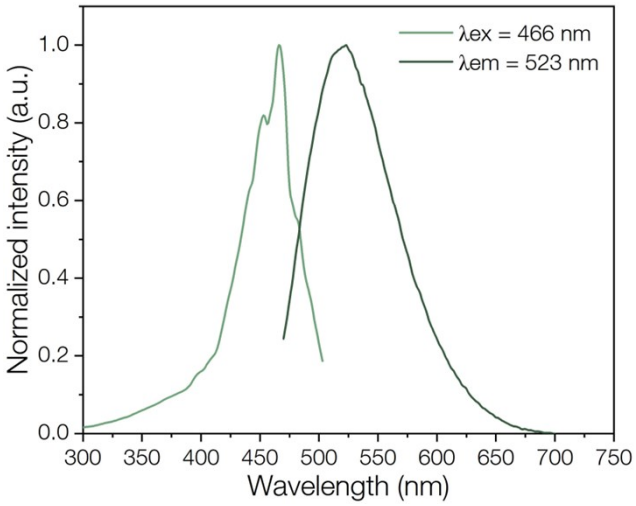

Fig. S6 Excitation and emission spectra of **1**.

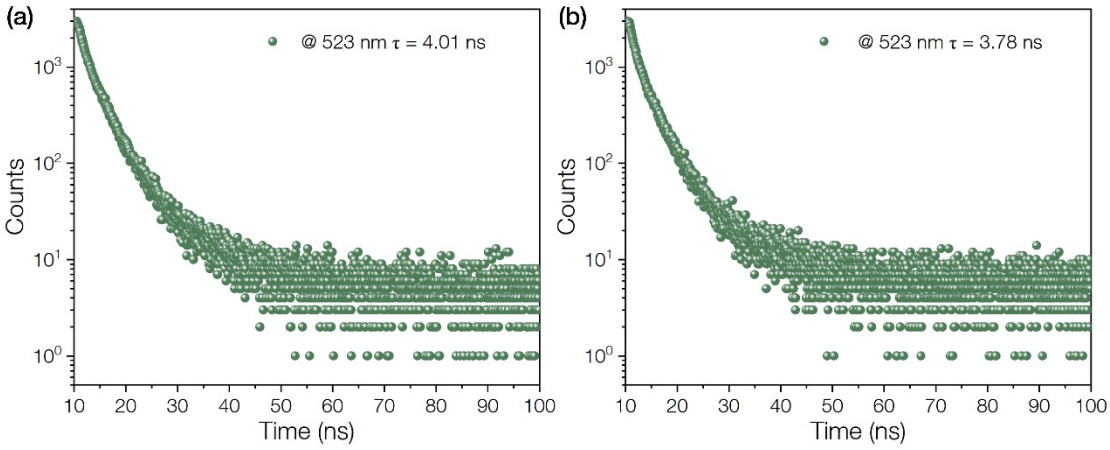

Fig. S7 The fluorescence lifetimes of **1** (a) and **1P** (b) at 523 nm.

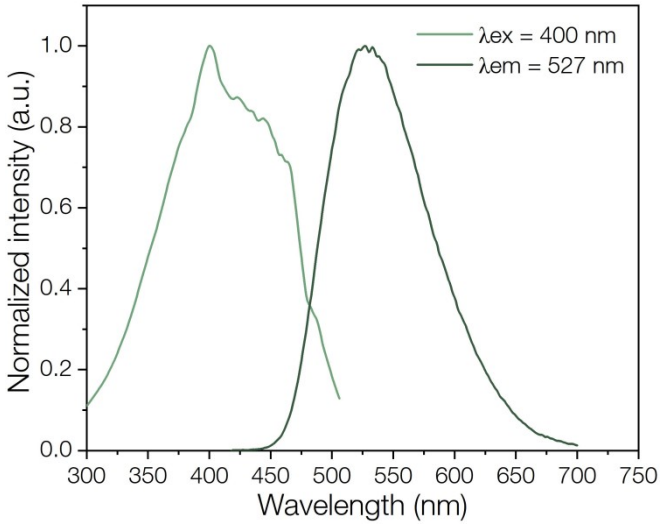

Fig. S8 Excitation and emission spectra of (**cbmby**)**Br**.

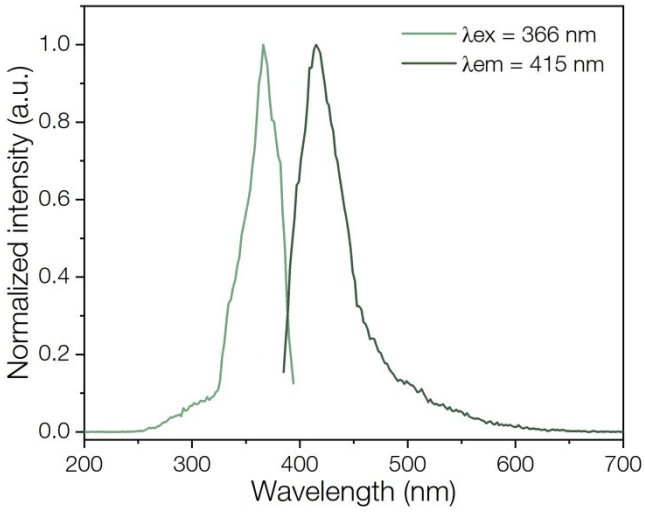

Fig. S9 Excitation and emission spectra of **H_4betc**.

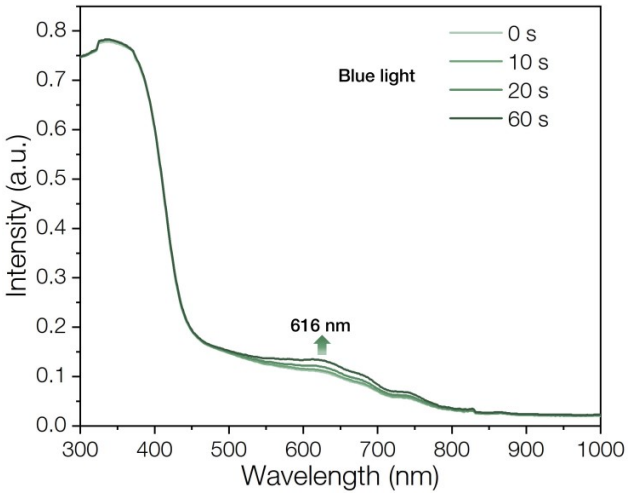

Fig. S10 UV/Vis diffuse reflectance spectrum of **1** under blue light.

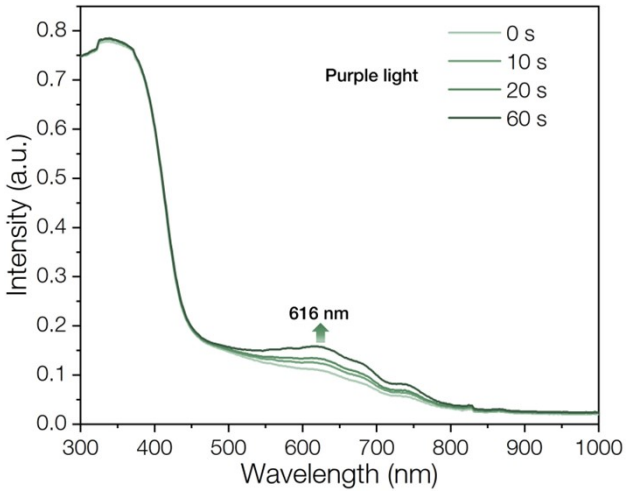

Fig. S11 UV/Vis diffuse reflectance spectrum of **1** under purple light.

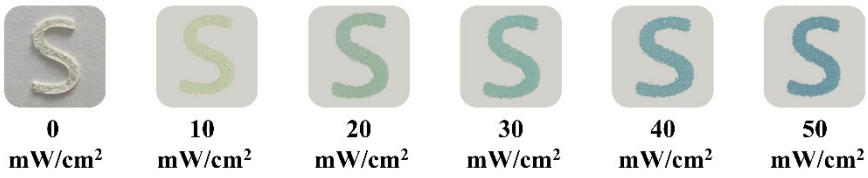

Fig. S12 Photographs indicating the different UV exposure levels (mW cm^{-2}) of **1** via different color changes.

3. Additional Table

Tab. S1 Crystal Data and Structure Refinements for **1.**

Empirical formula	**$C_{34}H_{25}N_2O_{11}$ (1)**
Formula	637.56
T (K)	273
Crystal system	monoclinic
Space group	$P2_1/c$
a (Å)	9.9821(6)
b (Å)	9.5637(6)
c (Å)	30.9166(19)
α (°)	90
β (°)	92.524(3)
γ (°)	90
V (Å^3)	2948.6(3)
Z	4
μ (mm^{-1})	0.109
D_c (g cm^{-3})	1.436
F(000)	1324.0
$R_1{}^a$ [$I > 2\sigma(I)$]	0.0929
$wR_2{}^b$ [$I > 2\sigma(I)$]	0.2345
goodness of fit	1.096
CCDC	2533236

^{a} $R_1 = \sum(F_o - F_c)/\sum F_o$; ^{b} $wR_2 = [\sum w(F_o^2 - F_c^2)^2/\sum w(F_o^2)^2]^{1/2}$.

Tab. S2 Selected bond lengths (Å) and angles (deg) for **1**.

bond lengths (Å)		**angles (deg)**	
O7-C34	1.273(4)	O7-C34-C27	116.1(3)
O8-C33	1.310(4)	O8-C33-C29	112.7(3)
O11-C32	1.290(5)	O3-C1-C2	117.8(6)
O5-C25	1.280(5)	C19-N1-C15	119.9(4)
O3-C1	1.221(9)	C19-N1-C14	120.8(4)
C27-C34	1.504(5)	C15-N1-C14	119.3(4)
C26-C31	1.387(5)	C28-C27-C34	119.3(3)
C20-C24	1.380(6)	C24-C20-C17	122.7(4)
N1-C19	1.329(6)	C23-C24-C20	119.5(4)
N1-C15	1.347(6)	N1-C19-C18	120.8(4)
N1-C14	1.503(6)	N2-C23-C24	123.0(4)
N2-C23	1.320(6)	N2-C22-C21	123.6(4)
N2-C22	1.321(6)	N1-C15-C16	120.8(4)

4. References

1 Y. Hua, Y. Shen, X. Meng, Y.-Y. Bai, Y.-F. Yang and H. Zhang, ACS Appl. Mater. Interfaces., 2025, 17, 55372-55379.

2 O. V. Dolomanov, L. J. Bourhis, R. J. Gildea, J. A. K. Howard and H. Puschmann, J. Appl. Crystallogr., 2009, 42, 339-341.

3 L.-J. Luan, Y. He, T. Wang, Z.-W. Liu, Acta Phys. Sin., 2021, 70, 166302.

4 B. Delley, J. Chem. Phys., 1990, 92, 508-517.

5 M. J. Frisch, G. W. Trucks, H. B. Schlegel, G. E. Scuseria, M. A. Robb, J. R. Cheeseman, G. Scalmani, V. Barone, G. A. Petersson, H. Nakatsuji, X. Li, M. Caricato, A. V. Marenich, J. Bloino, B. G. Janesko, R. Gomperts, B. Mennucci, H. P. Hratchian, J. V. Ortiz, A. F. Izmaylov, J. L. Sonnenberg, D. Williams-Young, F. Ding, F. Lipparini, F. Egidi, J. Goings, B. Peng, A. Petrone, T. Henderson, D. Ranasinghe, V. G. Zakrzewski, J. Gao, N. Rega, G. Zheng, W. Liang, M. Hada, M. Ehara, K. Toyota, R. Fukuda, J. Hasegawa, M. Ishida, T. Nakajima, Y. Honda, O. Kitao, H. Nakai, T. Vreven, K. Throssell, J. A. Montgomery, Jr., J. E. Peralta, F. Ogliaro, M. J. Bearpark, J. J. Heyd, E. N. Brothers, K. N. Kudin, V. N. Staroverov, T. A. Keith, R. Kobayashi, J. Normand, K. Raghavachari, A. P. Rendell, J. C. Burant, S. S. Iyengar, J. Tomasi, M. Cossi, J. M. Millam, M. Klene, C. Adamo, R. Cammi, J. W. Ochterski, R. L. Martin, K. Morokuma, O. Farkas, J. B. Foresman and D. J. Fox, Gaussian 16, Revision C.01, Gaussian, Inc., Wallingford, CT, 2016.

6 GaussView 6.0, R. Dennington, T. Keith, J. Millam, Semichem Inc., Shawnee Mission, KS, 2016.